Environmental Science & Technology

Article

Cite This: *Environ. Sci. Technol.* 2019, 53, 6887−6894

pubs.acs.org/est

Molecular-Level Characterization of Oil-Soluble Ketone/Aldehyde Photo-Oxidation Products by Fourier Transform Ion Cyclotron Resonance Mass Spectrometry Reveals Similarity Between Microcosm and Field Samples

Sydney F. Niles,[†,‡] Martha L. Chacón-Patiño,[‡] Huan Chen,[‡] Amy M. McKenna,[‡] Greg T. Blakney,[†] Ryan P. Rodgers,[*,‡,§] and Alan G. Marshall[*,†,‡]

[†]Department of Chemistry and Biochemistry, Florida State University, 95 Chieftain Way, Tallahassee, Florida 32306, United States

[‡]Ion Cyclotron Resonance Program, National High Magnetic Field Laboratory, Florida State University, Tallahassee, Florida 32310, United States

[§]Future Fuels Institute, Florida State University, 1800 East Paul Dirac Drive, Tallahassee, Florida 32310, United States

Supporting Information

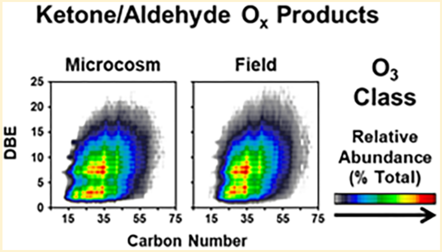

ABSTRACT: We present a solid-phase extraction method followed by derivatization with a charged tag to characterize ketone/aldehyde-containing functionalities (proposed photo-oxidation transformation products) in weathered petroleum by Fourier transform ion cyclotron resonance mass spectrometry (FT-ICR MS). A photo-oxidation-only microcosm mimics solar irradiation of crude oil in the environment after an oil spill. A biodegradation-only microcosm enables independent determination as to which of the two weathering processes contributes to the formation of oil-soluble ketone/aldehyde species. Results confirm that photo-oxidation produces ketones/aldehydes in crude oil when exposed to solar radiation in laboratory experiments, whereas biodegraded oil samples do not produce ketone/aldehyde compounds. Field samples collected after different time periods and locations after the Deepwater Horizon oil spill are also shown to contain ketones/aldehydes, and comparison of field and photo-oxidation-only microcosm transformation products reveal remarkable similarity. These results indicate that the photo-oxidation microcosm comprehensively represents ketone/aldehyde-formation products in the field, whereas the biodegradation microcosm does not. Solid-phase extraction coupled with derivatization leads to selective identification of ketone/aldehyde species by MS. Although improved dynamic range and slightly reduced mass spectral complexity is achieved by separation/derivatization, comprehensive molecular characterization still requires mass resolving power and mass accuracy provided by FT-ICR MS.

INTRODUCTION

The United States Department of Energy estimates that more than 1 million gallons of petroleum are spilled into United States waters from oil production facilities every year.[1] Major oil spills such as the *Deepwater Horizon* (DWH) (2010) and Taylor oil spill (2004 to the present day) further increase the amount of oil released into aquatic ecosystems.[2] Petroleum is one of the most complex naturally occurring mixtures, composed of a wide variety of chemical species of known toxicity.[3−6] Extensive research suggests that polycyclic aromatic hydrocarbons, which are abundant in petroleum, have carcinogenic effects in living organisms.[7] Therefore, a more detailed understanding of the transformation products of petroleum species upon release into aquatic ecosystems is critical for environmental science and health applications.

After release into the sea, petroleum undergoes chemical and physical changes evidenced by the appearance of oil mousses, mats, sheens, and slicks on the ocean surface and throughout marshes.[8−10] Physical differences between the unweathered crude oil and the weathered products suggest extensive changes in the molecular composition that may be caused by bio- and/or photo-oxidation.[11] Research efforts that target bio- and photo-oxidation of petroleum highlight the critical role of photo-oxidation and identify transformation products with multiple oxygen-containing functionalities.[12−15] Studies of model compounds demonstrate that sun-light irradiation of polycyclic aromatic hydrocarbons produces a plethora of oxidation products, including carboxylic acids, aldehydes, and ketones.[13,16−19] For instance, naphthalene irradiation can produce more than 20 unique transformation products, identified by gas chromatography and low-resolution mass spectrometry, and include diketones and oxygen-containing heterocycles that result from opening/closing reactions of the naphthalene ring system.[12,20] Moreover, in vitro studies suggest that polycyclic aromatic ketones have toxic effects in

Received: February 13, 2019
Revised: April 24, 2019
Accepted: May 20, 2019
Published: May 31, 2019

DOI: 10.1021/acs.est.9b00908

animals.[21] Therefore, a comprehensive characterization of the photo-oxidation products derived from petroleum spills, especially ketone/aldehyde-containing compounds, is of paramount importance for toxicological studies. However, molecular-level characterization of these products is difficult due to petroleum's complexity in composition, thermal lability, polarizability, and boiling point.[22−24]

Although preliminary studies relied on infrared (IR) spectroscopy and low-resolution mass spectrometry, recent advances in analytical techniques allow for enhanced understanding of photo-oxidation reactions. Specifically, Fourier-transform ion cyclotron resonance mass spectrometry (FT-ICR MS) has revealed the composition of samples collected after the DWH spill, because it identifies molecular elemental compositions for components of ultracomplex mixtures, irrespective of boiling point.[6] Post-DWH samples revealed oxygenated hydrocarbons such as hydroxyl and carboxylic acid functionalities selectively ionized by negative ion electrospray ionization (−) ESI, detected by FT-ICR MS. Positive ion (+) ESI with formic acid solvent modification at high concentration (up to 5%), also revealed a continuum of oxygenated compounds, which were hypothesized to contain ketones or aldehydes, and recognized as weakly basic oxygen functionalities.[25] Although two-dimensional gas chromatography time-of-flight (GC×GC TOF) analysis confirmed the presence of ketones, GC×GC is limited to the characterization of volatile species and therefore provides incomplete characterization of petroleum-derived samples.[25] The use of high formic acid concentration was suggested as an effective means to ionize ketones and aldehydes preferentially; however ketones cannot be unambiguously differentiated from other O-containing functionalities, such as alcohols and furans. Thus, techniques that can unambiguously detect ketone/aldehyde transformation products in weathered petroleum, irrespective of boiling point, and definitively confirm the process (bio- or photo-oxidation) that created them is fundamental for determining the long-term impact of DWH oil in coastal ecosystems. To identify ketone/aldehyde species in weathered oil transformation products, we apply a technique that isolates and tags ketone/aldehyde-containing compounds in petroleum[27] to field and laboratory-irradiated oil residues for subsequent FT-ICR MS analysis.

It is important to consider that incorporation of oxygen-containing functionalities in petroleum compounds through solar photo-oxidation can lead to solubility changes,[28] which are of substantial interest due to potential environmental and public health effects, because these compounds become increasingly water-soluble. Determining the processes that results in the presence of ketone/aldehyde-containing oil- and water-soluble compounds in the environment and the effect of sunlight on the transformation of petroleum species is critical to development of improved models to understand past spills and predict long-term impacts of future spills, and design efficient cleanup strategies.

Biodegradation of petroleum compounds occurs after oil is released into the environment, and also produces oxygenated hydrocarbons.[29] In field samples, it is not possible to discern which process, photo- or bio-oxidation, selectively produces oxygen-containing species, because the process(es) that produce them are pathway-dependent, and thus unknown. However, in laboratory microcosms, the relative contribution of each process (photo-only or bio-only) can be isolated and tied to specific degradation products.

The molecular composition of petroleum comprises a structural/compositional continuum in carbon number, aromaticity,[30−33] heteroatom content, and molecular motifs (e.g., single-core versus multicore structures).[34−36] Particularly, the continuous composition of oxygen-containing species is of major interest because these compounds have significant impact on petroleum solubility, aggregation, and emulsifying behavior.[17,37−46] Previous work demonstrated a continuum distribution of O_x species (e.g., O_1, O_2, O_3, O_4, O_5, O_6), in weathered DWH samples, accessible by both positive and negative ESI FT-ICR MS.[26,47] The negative-ion species were identified as hydroxy and carboxylic acid functionalities and the positive-ion species contained ketone functionalities, based on GC×GC time-of-flight mass spectrometry through previously established fragmentation pathways.[25] However, only some of the ions produced by (+) ESI are amenable to GC due to boiling point limitations, and therefore full characterization of the entire mass range was not possible. Furthermore, the boiling points of hydrocarbon compounds increase with the addition of oxygen atoms, limiting their GC-based access to only single oxygen-containing species below $\sim C_{30}$.[48] Because positive-ion ESI FT-ICR MS is amenable to characterization of the entire range of carbon number species (petroleum molecules may contain in excess of 100 carbons),[49] as well as compounds with high heteroatom content, these limitations may be overcome to better characterize ketone-containing species if isolated prior to high resolution mass spectral analysis.

Here, we use a solar simulator and the National Institute of Standards and Technology (NIST) Macondo well, Mississippi Canyon (MC) Block 252 Gulf of Mexico crude oil,[50] to compare the molecular composition determined by FT-ICR MS of oil spill field samples and lab-irradiated samples. Oil compounds derived from field and laboratory samples are first fractionated by strong anion exchange (SAX) solid phase extraction (SPE) to enrich ketones/aldehydes. Ketones/aldehydes are then derivatized by use of a charged tag that selectively modifies ketone/aldehyde-containing compounds during subsequent FT-ICR MS analysis.[27,51] In addition, ketone/aldehyde compounds isolated from a biodegradation-only (bio-only) microcosm is compared to field and photo-only oil compounds. Molecular-level analysis reveals the carbon number distribution and degree of aromaticity (double bond equivalents (DBE) = number of rings plus double bonds to carbon), derived from the molecular elemental composition,[52] whereas previous studies accessed only the small fraction amenable to GC analysis. Furthermore, extensive lab-conducted biodegradation does not appear to produce abundant oil-soluble ketone/aldehyde species and exhibits a different composition than field samples. Comparison of transformation products formed in the photo-only microcosm to field samples highlights the structural similarity between ketone/aldehydes, and strongly suggests that photo-oxidation is the dominant mechanism for formation of oxygenated hydrocarbons in weathered DWH oil.

High resolution FT-ICR MS analysis uniquely determines the elemental composition of thousands of compounds in complex matrices through exact mass measurement, Kendrick mass defect, and isotopic fine structure.[53,54] The thousands of elemental compositions identified from a single mass spectrum, can be sorted according to heteroatom class (e.g., those compounds that each contain carbon, hydrogen, two nitrogen atoms, and one oxygen atom define the N_2O_1 heteroatom

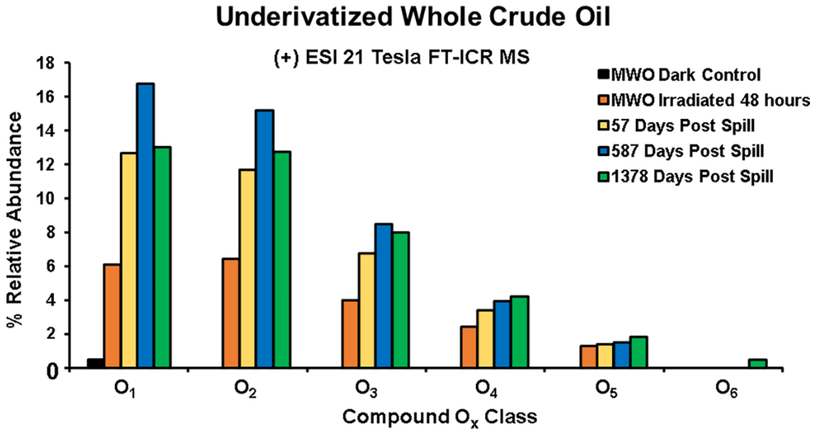

Figure 1. Heteroatom O_x class relative abundance distribution for lab-irradiated (orange), dark control (black), and three replicate field samples (yellow, blue, green) of Gulf of Mexico Crude Oil (SRM 2779) (Macondo Wellhead Oil, MWO). The lab-irradiated and field samples exhibit higher relative abundances of oxygen-containing compounds as well as an increased number of oxygen-atoms relative to the dark control. The class distribution does not reveal the functionality of the oxygen-containing species.

class), number of carbon atoms, and double bond equivalents (DBE). Moreover, for a given heteroatom class, an isoabundance-contoured plot of DBE vs carbon number provides a fingerprint that combines molecular size (from carbon number) and aromaticity (from DBE), which can be useful in predicting a variety of behaviors, such as emulsion stability.[55]

EXPERIMENTAL METHODS

Field Samples. Gulf of Mexico Crude Oil (SRM 2779) (Macondo Well Oil, MWO) was purchased from the National Institute of Standards and Technology (NIST, Gaithersburg, MD). Three field samples were used in this study: (1) an offshore floating oil mat collected near Pensacola, FL (30.068° N, 86.89° W) on June 10, 2010 (57 days after the initial spill, and before the well was capped); (2) sand patty collected in Gulf Shores, AL (30.25° N, 87.69° W) on November 27, 2011 (586 days postspill); and (3) rock scraping collected on Dauphin Island, AL on January 27, 2014 (1368 days postspill). Samples were placed in precombusted glass containers, transported on ice for one to three days, and then stored at −20 °C until further analysis. Approximately 20 g of oiled sand from each location was homogenized with an equal weight of sodium sulfate drying agent, loaded into a 30 × 100 mm^2 cellulose thimble, Soxhlet-extracted with 90:10 (v/v) toluene/methanol for 12 h and desolvated under dry nitrogen (N_2). Oiled extracts not consumed in this study remain preserved for future studies. Amplifex Keto-Reagent was obtained from AB Sciex (Framingham, MA). All solvents were HPLC grade from JT Baker chemicals (Phillipsburg, PA) and used as-received. All glassware was acid-washed and subjected to a Thermo Scientific Lindberg/Blue M Moldatherm box furnace (BF51828C-1, Thermo Scientific, U.S.A.) at 550 °C for 4 h for combustion of any organic material prior to experiments.

Solar Simulation Microcosm. A thin oil film (120 μm) generated with 325 mg (385 μL) oil was layered onto 50 mL autoclaved 70% artificial seawater (Instant Ocean Aquarium Systems, Inc., Mentor, OH, U.S.A.) in a jacketed beaker attached to a water chiller.

Samples were subsequently placed in an ATLAS Suntest CPS solar simulator, where they were irradiated by artificial sunlight for 48 h (equivalent to 12 days of natural sunlight[22]) at 27 °C. A dark control was covered with aluminum foil and allowed to stir for 48 h for comparison with the irradiated sample. After irradiation, water was removed by pipet and the oil layer was isolated and dried under nitrogen gas.

Biodegradation Microcosm. Biodegradation experiments were conducted with a microbial population isolated from live seawater collected from the Gulf of Mexico (29.91 N, 84.51 W); (temperature 23.1 °C; salinity 30.8 parts per thousand; pH 7.6; dissolved oxygen 5.21 mg L^{-1}). Samples were stored for 3 h during transport the National High Magnetic Field Laboratory (Tallahassee, FL), where they were filtered and stored. Filtration was performed with a 0.8 μm membrane filter to remove debris and large organisms. Additional filtration with a 0.2 μm membrane filter allowed for isolation of the microbial population. The microbial population was then added to sterile artificial seawater. Crude oil (325 mg) was then added to the biomicrocosm to generate an oil film of the same thickness as for the photo-oxidation microcosm. The biomicrocosm was wrapped in aluminum foil to prevent photo-oxidation and incubated (Thermo Scientific MaxQ 4000 orbital shaker) while shaken at 110 rpm at 23 °C for 30 days. The sample was monitored every 10 days throughout incubation. After 30 days, 5 mL of toluene was added to the sample to dissolve oil, shaken, and the oil layer was isolated by glass pipet. The sample was subsequently dried under nitrogen gas and stored in the dark at 4 °C to prevent further oxidation of samples prior to mass analysis.

Ketone Isolation. The lab-simulated photo-oxidized oil, a dark control, and three different field samples were then subjected to a previously reported ketone isolation method which has been previously developed (Figure S1 of the Supporting Information, SI). A strong anion exchange (SAX) solid phase extraction cartridge (Agilent Bond Mega BE-SAX) separated compounds based on polarity, and yielded 3 fractions: unmodified oil (pentane), ketone and aldehyde fraction (DCM), and carboxylic acids (methanol).[51] Approximately 15 mL of each solvent was used to elute fractions.

Ketone/Aldehyde Derivatization. The ketone and aldehyde-containing dichloromethane (DCM) fraction was then reconstituted in toluene (1 mg/mL) and derivatized for FT-ICR MS analysis. For derivatization, the ketone/aldehyde fractions (dissolved in 200 μL toluene) were added to 200 μL of the charged tag (Amplifex Keto Reagent—see below)

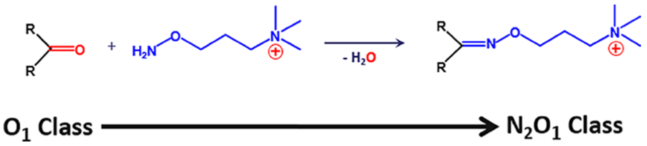

and mixed for 1 h at ambient temperature.[27] Samples were subsequently dried under nitrogen gas and stored in a dark fridge at 4 °C.

FT-ICR MS Analysis. All samples were dissolved in toluene, and further diluted in methanol to a final concentration of 250 μg/mL prior to analysis by (+) ESI FT-ICR MS. Underivatized crude oil samples were spiked with 4% formic acid prior to analysis, whereas derivatized crude oil samples were analyzed without solvent modifier. Samples were then infused at 0.5 μL/min for (+) ESI 21 T FT-ICR MS analysis, as described previously.[53] Molecular assignments were performed by Predator[56] and PetroOrg computer software.[57]

■ RESULTS AND DISCUSSION

Detection of O_x Compounds by Positive-Ion ESI. Heteroatom class distributions determined by positive-ion ESI FT-ICR MS (Figure 1) report higher relative abundances for O_x heteroatom classes detected in field samples and laboratory-irradiated oil compared to the dark control, which contains only O_1 species. However, the laboratory-irradiated and field samples contain abundant O_1−O_5 compounds, with a higher relative abundance for O_x species in field samples than in the laboratory-irradiated sample. For both field and laboratory-irradiated samples, a continuous distribution of O-containing species, from O_1 to O_5 is observed. Furthermore, the lower relative abundance of O_x species in lab-irradiated samples is consistent with their irradiation periods, because the field samples were likely exposed to sunlight for several months, or even years. The most heavily weathered field sample (collected 27 January 2014, 1368 days post spill), was the only sample for which O_6 species were detected in appreciable amount. However, the chemical functionality of these basic O_x species not detected in the parent oil remains unclear based simply on analysis of the whole oil samples.

Assigned molecular formulas for the O_1, O_2, and O_3 classes detected in field and laboratory-irradiated samples, determined by (+) ESI 21 T FT-ICR MS, are converted to graphical images of DBE vs carbon number plots in Figure 2, which reveals the presence of O_x compounds that span a wide range of carbon number and DBE (aromaticity). Moreover, the lab-irradiated samples contain low carbon number species (down to carbon number 12 for O_1), whereas the field samples lack low carbon number species (O_1 containing-compounds begin at C_{18}, C_{15}, and C_{16} for the three field samples). Thus, to determine whether or not ketone- and/or aldehyde-containing species are formed through photo-oxidation reactions, and to mitigate limited characterization that results from selective ionization, field and lab-irradiated samples were fractionated by a SAX method and derivatized prior to MS analysis.

Derivatization of Ketone/Aldehyde Species. A previously developed SAX method was shown to effectively isolate ketone/aldehyde containing species for petroleum, as confirmed by the use of a derivatization agent prior to (+) ESI FT-ICR MS analysis.[51] Although originally developed to analyze naphthenic acid degradation products for corrosion studies, the method is also effective for isolation of ketone-containing species in petroleum samples. Note that the above derivatization agent does not differentiate between aldehyde- and ketone-containing species.

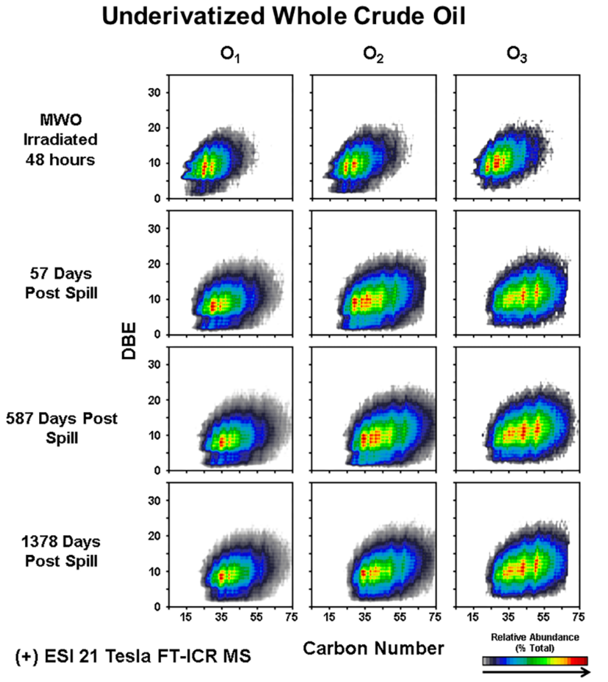

Figure 2. Isoabundance-contoured plots of double bond equivalents (DBE) vs carbon number for lab-irradiated MWO and three replicate field samples for the O_1−O_3 classes. Although all samples span similar carbon-number and DBE ranges, the lab-irradiated sample exhibits lower relative abundances of the lowest-DBE species in the field samples.

Detection of Ketone/Aldehyde Compounds. Isolation and derivatization of ketone/aldehyde-containing species results in higher relative abundance of the O_1−O_5 classes for the field and laboratory-irradiated samples. Figure 3 shows the increased relative abundance of ketone-containing oxygen species for the laboratory-irradiated samples relative to the dark control, (see Figure S2). The dark sample exhibits low relative abundance of O_1 and O_2 species, whereas the irradiated samples are enriched with O_1−O_5 ketone/aldehyde-containing compounds. Furthermore, ketone/aldehyde-containing field samples exhibit an O_x distribution similar to that for the lab-irradiated sample. The oxygen continuum observed for ketone/aldehyde-containing lab-irradiated and field samples resembles the oxygen continuum accessed by positive-ion ESI with high formic acid concentration (Figure 1).

For comparison with photo-oxidized oil, biodegraded Macondo well oil (MWO) was also SAX-fractionated, derivatized, and analyzed by ultrahigh-resolution MS. Biodegraded species exhibit significantly lower abundance of O_1−O_4 species (Figure 3), suggesting that biodegradation does not lead to ketone/aldehyde-formation.

These results suggest that photo-oxidation of petroleum produces ketones/aldehydes, in agreement with reports of sunlight oxidation of petroleum model compounds,[12,58] whereas biodegradation does not play a critical role in producing ketone/aldehyde functionalities. The similarity between field samples and lab-irradiated samples points to photo-oxidation

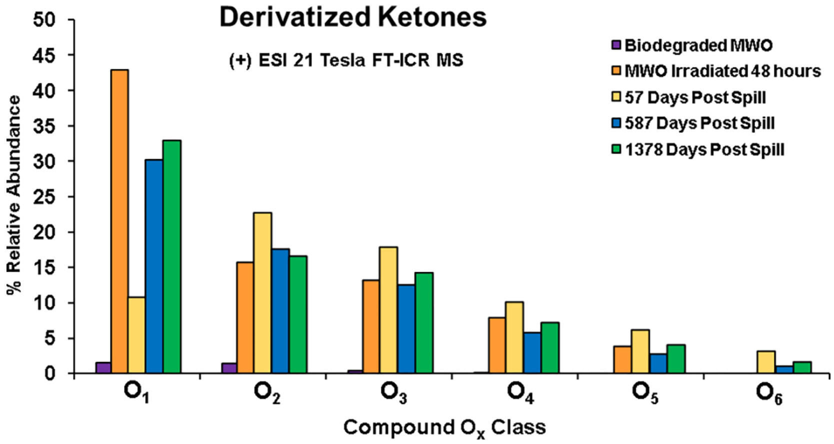

Figure 3. Relative abundance distribution throughout the O_1-O_6 classes for the derivatized ketone/aldehyde-containing fraction of biodegraded MWO (purple), lab-irradiated MWO (orange), as well as three replicate field samples (yellow, blue, and green). Higher relative abundances of ketone/aldehyde-containing species is observed for the three field samples and lab-irradiated sample than for to the biodegraded oil. Furthermore, the biodegraded oil lacks appreciable ketone-containing species with more than four oxygen atoms.

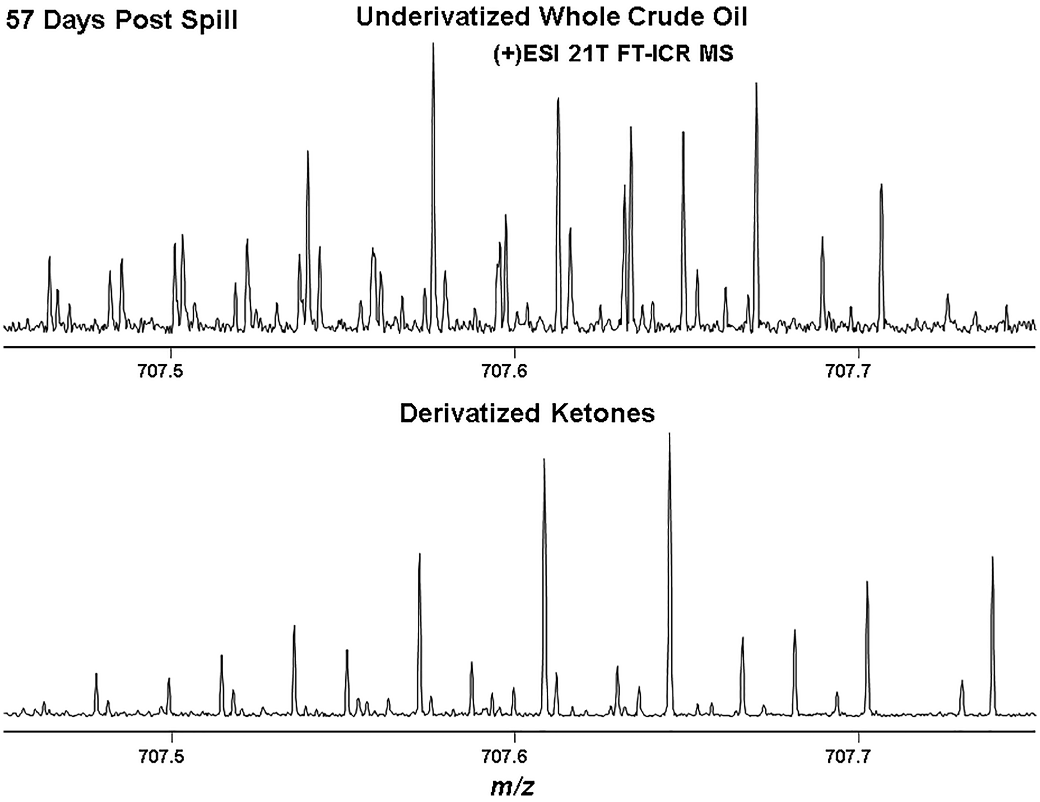

Figure 4. Mass scale-expanded (+) ESI-derived 21 T FT-ICR mass spectra for underivatized whole crude oil and the derivatized ketone/aldehyde fraction for a field sample collected on June 16, 2010. The derivatized ketone sample exhibits higher signal-to-noise ratio than the whole sample.

as an important source of ketone/aldehyde formation in weathered petroleum. Moreover, the significantly lower relative abundance of ketone/aldehyde species in biodegraded oil suggests that photo-oxidation is the dominant mechanism in the formation of oil soluble ketone/aldehyde-containing transformation products derived from the *Deepwater Horizon* oil spill.

Additional data processing was conducted to account for the derivatization tag. Heteroatom class plots are labeled to indicate O_1-O_5 species, whereas $N_2O_1-N_2O_5$ classes were assigned from the ICR mass spectral data and N_2 was manually removed from N_2O_x assignments due to the derivatization tag. Furthermore, for DBE vs carbon number plots for derivatized samples, the molecular assignments were shifted by 6 carbons to the left to account for 6 extra carbons introduced by derivatization. The charged derivatization tag removes the need for a protonation modifier for electrospray ionization and provides preferential analysis of ketones/aldehydes relative to other compounds in the sample, therefore reducing chemical noise.

Molecular-Level Comparison of Field vs Microcosm. The FT-ICR MS signal-to-noise ratio is significantly higher for the isolated and derivatized ketone/aldehyde-containing fraction, as seen for a mass scale-expanded 0.3 Da segment

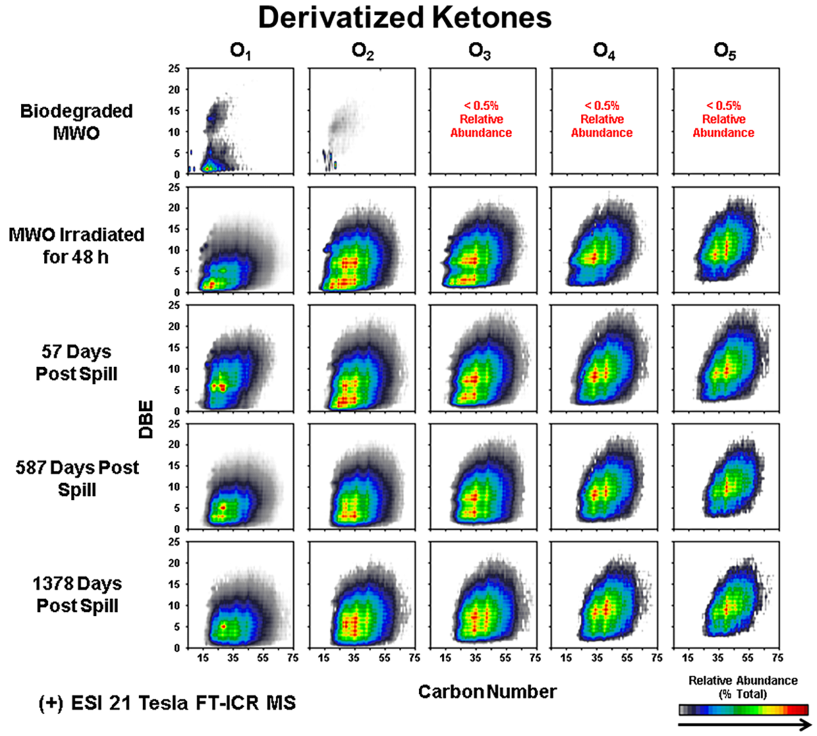

Figure 5. DBE vs carbon number plots for the derivatized ketone/aldehyde fraction for biodegraded MWO, lab-irradiated MWO, and three replicate field samples. The biodegraded MWO occupies a completely different compositional space. The photo-oxidation microcosm therefore better replicates hydrocarbon ketone-formation in the environment than the biodegradation microcosm.

at nominal mass at 707 Da (Figure 4). The broadband mass spectrum of the underivatized crude oil from a field sample collected on 16 June 2010 for $707 < m/z < 708$ exhibits 27 015 resolved peaks vs 22 546 for the DCM/derivatized fraction for the same sample. Although the number of species detected for the two samples is comparable, the separated/derivatized sample maximum S/N in Figure 4 is ~3-fold higher for the DCM/derivatized fraction (~202) than the underivatized whole crude oil (~70). In any case, the weathered petroleum samples are still compositionally complex and extend to relatively high molecular weight. Therefore, reliable molecular information for these samples is accessible only by ultrahigh-resolution high-field FT-ICR MS.

Plots of DBE vs carbon number are displayed in Figure 5 for derivatized biodegraded, lab-irradiated, and field samples from the dichloromethane (DCM) fraction. The lab-irradiated oil sample and the weathered field samples span remarkably similar carbon number and DBE ranges. Conversely, the biodegraded oil exhibits a completely different compositional profile, further indicating that biodegradation does not lead to the formation of oil-soluble ketone/aldehyde-containing species. Thus, the current results suggest that photoirradiation generates abundant, oil-soluble, ketone-containing transformation products similar to those identified in field samples.

Concluding Remarks. Samples from the photo-oxidation microcosm and those collected in the field exhibit higher relative abundance of oxygen-containing species than that of a dark control, and display an O_x continuum similar to those previously reported for weathered oil.[25] Ketones and aldehydes can be successfully isolated and identified by FT-ICR MS in field samples collected after DWH. Although these functionalities typically comprise a small fraction of unweathered/virgin crude oil, we show that they form in high relative abundance through photo-oxidation in the laboratory. Furthermore, a separation and derivatization method allows for observation of ketone/aldehyde species in both lab-irradiated and field samples. The ketone/aldehyde fractions from lab-irradiated and field samples share remarkable similarity in terms of carbon number and DBE range, as well as relative abundances of O_x ketone/aldehyde species. A biodegradation microcosm yields no oil-soluble transformation products that resemble field samples collected after the DWH spill. Collectively, these results suggest that photo-oxidation constitutes the dominant mechanism in production of oil-soluble ketone/aldehyde-containing species in weathered petroleum.

■ ASSOCIATED CONTENT

Ⓢ Supporting Information

The Supporting Information is available free of charge on the ACS Publications website at DOI: 10.1021/acs.est.9b00908.

> SPE method based on strong-anion exchange to separate petroleum species by polarity to allow for isolation of the ketone/aldehyde fraction prior to derivatization and analysis by (+) ESI 21T FT-ICR MS (Figure S1) and lab-irradiated derivatized ketone/aldehyde fraction for the photoirradiation microcosm (Figure S2) (PDF)

■ AUTHOR INFORMATION

Corresponding Authors

*Tel: 850-644-2398; fax: +1-850-644-1366; e-mail: rodgers@magnet.fsu.edu.
*Tel: +1-850-644-0529; fax: +1-850-644-1366; e-mail: marshall@magnet.fsu.edu.

ORCID

Amy M. McKenna: 0000-0001-7213-521X

Greg T. Blakney: 0000-0002-4205-9866
Ryan P. Rodgers: 0000-0003-1302-2850
Alan G. Marshall: 0000-0001-9375-2532

Notes

The authors declare no competing financial interest.

ACKNOWLEDGMENTS

The authors thank Chad R. Weisbrod and Don F. Smith for their assistance in data collection and instrument performance. The authors also thank Yuri E. Corilo for assistance with PetroOrg software and Cameron A. Davis for field sample extraction prior to analysis. This research was made possible in part by a grant from The Gulf of Mexico Research Initiative, and in part by National Science Foundation Cooperative Agreement No. DMR-1644779, the Florida State University Future Fuels Institute, and the State of Florida. Data are publicly available through the Gulf of Mexico Research Initiative Information & Data Cooperative (GRIIDC) at https://data.gulfresearchinitiative.org (doi: 10.7266/n7-jdr0-dz24, 10.7266/n7-mpw7-rx40, 10.7266/n7-3d8b-0860).

REFERENCES

(1) Patterson, L. A.; Konschnik, K. E.; Wiseman, H.; Fargione, J.; Maloney, K. O.; Kiesecker, J.; Nicot, J.; Baruch-mordo, S.; Entrekin, S.; Trainor, A.; Saiers, J. E. Unconventional Oil and Gas Spills: Risks, Mitigation Priorities, and State Reporting Requirements. *Environ. Sci. Technol.* **2017**, *51* (5), 2563−2573.

(2) McNutt, M. K.; Camilli, R.; Crone, T. J.; Guthrie, G. D.; Hsieh, P. A.; Ryerson, T. B.; Savas, O.; Shaffer, F. Review of flow rate estimates of the Deepwater Horizon oil spill. *Proc. Natl. Acad. Sci. U. S. A.* **2012**, *109* (50), 20260−20267.

(3) Frank, R. A.; Fischer, K.; Kavanagh, R.; Burnison, B. K.; Arsenault, G.; Headley, J. V.; Peru, K. M.; Van Der Kraak, G.; Solomon, K. R. Effect of Carboxylic Acid Content on the Acute Toxicity of Oil Sands Naphthenic Acids. *Environ. Sci. Technol.* **2009**, *43* (2), 266−271.

(4) Incardona, J. P.; Swarts, T. L.; Edmunds, R. C.; Linbo, T. L.; Aquilina-beck, A.; Sloan, C. A.; Gardner, L. D.; Block, B. A.; Scholz, N. L. Exxon Valdez to Deepwater Horizon: Comparable toxicity of both crude oils to fish early life stages. *Aquat. Toxicol.* **2013**, *142−143*, 303−316.

(5) Xu, E. G.; Mager, E. M.; Grosell, M.; Pasparakis, C.; Schlenker, L. S.; Stieglitz, J. D.; Benetti, D.; Hazard, E. S.; Courtney, S. M.; Diamante, G.; Freitas, J.; Hardiman, G.; Schlenk, D. Time- and Oil-Dependent Transcriptomic and Physiological Responses to Deepwater Horizon Oil in Mahi-Mahi (Coryphaena hippurus) Embryos and Larvae. *Environ. Sci. Technol.* **2016**, *50* (14), 7842−7851.

(6) Xu, E. G.; Khursigara, A. J.; Magnuson, J.; Hazard, E. S.; Hardiman, G.; Esbaugh, A. J.; Roberts, A. P.; Schlenk, D. Larval Red Drum (Sciaenops ocellatus) Sublethal Exposure to Weathered Deepwater Horizon Crude Oil: Developmental and Transcriptomic Consequences. *Environ. Sci. Technol.* **2017**, *51* (17), 10162−10172.

(7) USEPA. *Provisional Guidance for Quantitative Risk Assessment of Polycyclic Aromatic Hydrocarbons*; 1993.

(8) Liu, Z.; Liu, J.; Zhu, Q.; Wu, W. The weathering of oil after the Deepwater Horizon oil spill: Insights from the chemical composition of the oil from the sea surface, salt marshes and sediments. *Environ. Res. Lett.* **2012**, *7* (3), 1−14.

(9) Liu, Z.; Liu, J.; Gardner, W. S.; Shank, G. C.; Ostrom, N. E. The impact of Deepwater Horizon oil spill on petroleum hydrocarbons in surface waters of the northern Gulf of Mexico. *Deep Sea Res., Part II* **2016**, *129*, 292−300.

(10) Gustitus, S. A.; Clement, T. P. Formation, Fate, and Impacts of Microscopicand Macroscopic Oil-Sediment Residuesin Nearshore Marine Environments: A Critical Review. *Rev. Geophys.* **2017**, *55* (4), 1130−1157.

(11) Nicodem, D. E.; Fernandes, M. C. Z.; Guedes, C. L. B.; Correa, R. J. Photochemical processes and the environmental impact of petroleum spills. *Biogeochemistry* **1997**, *39* (2), 121−138.

(12) Mcconkey, B. J.; Hewitt, L. M.; Dixon, D. G.; Greenberg, B. M. NATURAL SUNLIGHT INDUCED PHOTOOXIDATION OF NAPHTHALENE IN AQUEOUS SOLUTION. *Water, Air, Soil Pollut.* **2002**, *136* (1/4), 347−359.

(13) Palen, E. J.; Allen, D. T.; Pandis, S. N.; Paulson, S. E.; Seinfeld, J. H.; Flagan, R. C. FOURIER TRANSFORM INFRARED ANALYSIS OF AEROSOL FORMED IN THE PHOTO-OXIDATION OF ISOPRENE AND B-PINENE. *Atmos. Environ., Part A* **1992**, *26A* (7), 1239−1251.

(14) Aeppli, C.; Swarthout, R. F.; O'Neil, G. W.; Katz, S. D.; Nabi, D.; Ward, C. P.; Nelson, R. K.; Sharpless, C. M.; Reddy, C. M. How Persistent and Bioavailable Are Oxygenated Deepwater Horizon. *Environ. Sci. Technol.* **2018**, *52* (13), 7250−7258.

(15) Cao, X.; Tarr, M. A. Aldehyde and Ketone Photoproducts from Solar-Irradiated Crude Oil-Seawater Systems Determined by Electrospray Ionization-Tandem Mass Spectrometry. *Environ. Sci. Technol.* **2017**, *51* (20), 11858−11866.

(16) Takekawa, H.; Minoura, H.; Yamazaki, S. Temperature dependence of secondary organic aerosol formation by photo-oxidation of hydrocarbons. *Atmos. Environ.* **2003**, *37*, 3413−3424.

(17) Bobinger, S.; Andersson, J. T. Photooxidation products of polycyclic aromatic compounds containing sulfur. *Environ. Sci. Technol.* **2009**, *43* (21), 8119−8125.

(18) Ehrhardt, M. Photo-Oxidation Products of Fossil Fuel Components in the Water of Hamilton Harbour, Bermuda. *Mar. Chem.* **1987**, *22*, 85−94.

(19) Boukir, A.; Guiliano, M.; Asia, L.; El Hallaoui, A.; Mille, G. A fraction to fraction study of photo-oxidation of BAL 150 crude oil asphaltenes. *Analusis* **1998**, *26* (9), 358−364.

(20) Chen, C.; Li, L.; Tang, P.; Cocker, D. R. SOA formation from photooxidation of naphthalene and methylnaphthalenes with m -xylene and surrogate mixtures. *Atmos. Environ.* **2018**, *180*, 256−264.

(21) Machala, M.; Ciganek, M.; Neca, J.; Pencikova, K.; Palkova, L.; Vondracek, J.; Loffler, I.; Streck, G.; Reifferscheid, G.; Fluckiger-Isler, S.; Weiss, J. M.; Lamoree, M.; Brack, W.; Lübcke-von Varel, U. Polar Compounds Dominate in Vitro Effects of Sediment Extracts. *Environ. Sci. Technol.* **2011**, *45* (6), 2384−2390.

(22) King, S. M.; Leaf, P. A.; Olson, A. C.; Ray, P. Z.; Tarr, M. A. Photolytic and photocatalytic degradation of surface oil from the Deepwater Horizon spill. *Chemosphere* **2014**, *95*, 415−422.

(23) Harriman, B. H.; Zito, P.; Podgorski, D. C.; Tarr, M. A.; Suflita, J. M. Impact of Photooxidation and Biodegradation on the Fate of Oil Spilled during the Deepwater Horizon Incident: Advanced Stages of Weathering. *Environ. Sci. Technol.* **2017**, *51* (13), 7412−7421.

(24) Ward, C. P.; Sharpless, C. M.; Valentine, D. L.; French-McCay, D. P.; Aeppli, C.; White, H. K.; Rodgers, R. P.; Gosselin, K. M.; Nelson, R. K.; Reddy, C. M. Partial Photochemical Oxidation Was a Dominant Fate of Deepwater Horizon Surface Oil. *Environ. Sci. Technol.* **2018**, *52* (4), 1797−1805.

(25) Ruddy, B. M.; Huettel, M.; Kostka, J. E.; Lobodin, V. V.; Bythell, B. J.; McKenna, A. M.; Aeppli, C.; Reddy, C. M.; Nelson, R. K.; Marshall, A. G.; Rodgers, R. P. Targeted petroleomics: Analytical investigation of macondo well oil oxidation products from pensacola beach. *Energy Fuels* **2014**, *28* (6), 4043−4050.

(26) Chen, H.; Hou, A.; Corilo, Y. E.; Lin, Q.; Lu, J.; Mendelssohn, I. A.; Zhang, R.; Rodgers, R. P.; McKenna, A. M. 4 years after the deepwater horizon spill: Molecular transformation of Macondo well oil in Louisiana salt marsh sediments revealed by FT-ICR mass spectrometry. *Environ. Sci. Technol.* **2016**, *50* (17), 9061−9069.

(27) Alhassan, A.; Andersson, J. T. Ketones in Fossil Materials—A Mass Spectrometric Analysis of a Crude Oil and a Coal Tar. *Energy Fuels* **2013**, *27* (10), 5770−5778.

(28) Ray, P. Z.; Chen, H.; Podgorski, D. C.; McKenna, A. M.; Tarr, M. A. Sunlight creates oxygenated species in water-soluble fractions of Deepwater horizon oil. *J. Hazard. Mater.* **2014**, *280*, 636−643.

(29) Atlas, R. M.; Hazen, T. C. Oil Biodegradation and Bioremediation: A Tale of the Two Worst Spills in U. S. History. *Environ. Sci. Technol.* **2011**, *45* (16), 6709−6715.

(30) Boduszynski, M. M. Composition of Heavy Petroleums. 1. Molecular Weight, Hydrogen Deficiency, and Heteroatom Concentration as a Function of Atmospheric Equivalent Boiling Point up to 1400 °F (760 °C). *Energy Fuels* **1987**, *1* (1), 2−11.

(31) Altgelt, K. H.; Boduszynski, M. M. Composition of Heavy Petroleums. 3. An Improved Boiling-Point Molecular-Weight Relation. *Energy Fuels* **1992**, *6* (1), 68−72.

(32) Boduszynski, M. M. In *Chemistry of Asphaltenes*; American Chemical Society: Washington, DC, 1982; pp 119−135.

(33) Boduszynski, M. M.; Altgelt, K. H. Composition of Heavy Petroleums. 4. Significance of the Extended Atmospheric Equivalent Boiling Point (AEBP) Scale. *Energy Fuels* **1992**, *6* (1), 72−76.

(34) Chacón-Patiño, M. L.; Rowland, S. M.; Rodgers, R. P. Advances in Asphaltene Petroleomics. Part 1: Asphaltenes Are Composed of Abundant Island and Archipelago Structural Motifs. *Energy Fuels* **2017**, *31* (12), 13509−13518.

(35) Chacón-Patiño, M. L.; Rowland, S. M.; Rodgers, R. P. Advances in Asphaltene Petroleomics. Part 2: Selective Separation Method That Reveals Fractions Enriched in Island and Archipelago Structural Motifs by Mass Spectrometry. *Energy Fuels* **2018**, *32* (1), 314−328.

(36) Chacón-Patiño, M. L.; Rowland, S. M.; Rodgers, R. P. Advances in Asphaltene Petroleomics. Part 3. Dominance of Island or Archipelago Structural Motif Is Sample Dependent. *Energy Fuels* **2018**, *32* (9), 9106−9120.

(37) Muller, H.; Pauchard, V. O.; Hajji, A. A. Role of Naphthenic Acids in Emulsion Tightness for a Low Total Acid Number (TAN)/High Asphaltenes Oil: Characterization of the Interfacial Chemistry. *Energy Fuels* **2009**, *23*, 1280−1288.

(38) Hansen, H. P. PHOTOCHEMICAL DEGRADATION OF PETROLEUM HYDROCARBON SURFACE FILMS ON SEAWATER. *Mar. Chem.* **1975**, *3*, 183−195.

(39) Charrié-Duhaut, A.; Lemoine, S.; Adam, P.; Connan, J.; Albrecht, P. Abiotic oxidation of petroleum bitumens under natural conditions. *Org. Geochem.* **2000**, *31* (10), 977−1003.

(40) Clingenpeel, A. C.; Rowland, S. M.; Corilo, Y. E.; Zito, P.; Rodgers, R. P. Fractionation of Interfacial Material Reveals a Continuum of Acidic Species That Contribute to Stable Emulsion Formation. *Energy Fuels* **2017**, *31* (6), 5933−5939.

(41) Giraldo-Dávila, D.; Chacón-Patiño, M. L.; McKenna, A. M.; Blanco-Tirado, C.; Combariza, M. Y. Correlations between Molecular Composition and Adsorption, Aggregation, and Emulsifying Behaviors of PetroPhase 2017 Asphaltenes and Their Thin-Layer Chromatography Fractions. *Energy Fuels* **2018**, *32* (3), 2769−2780.

(42) Qiao, P.; Harbottle, D.; Tchoukov, P.; Wang, X.; Xu, Z. Asphaltene Subfractions Responsible for Stabilizing Water- in-Crude Oil Emulsions. Part 3: Effect of Solvent Aromaticity Asphaltene Subfractions Responsible for Stabilizing Water-in- Crude Oil Emulsions. Part 3: Effect of Solvent Aromaticity. *Energy Fuels* **2017**, *31* (9), 9179−9187.

(43) Rojas-Ruiz, F. A.; Rueda, M. F.; Pachón-Contreras, Z.; Villar-García, Á.; Gómez-Escudero, A.; Orrego-Ruiz, J. A. Composition to Interfacial Activity Relationship Approach of Petroleum Sulfonates by Fourier Transform Ion Cyclotron Resonance Mass Spectrometry. *Energy Fuels* **2016**, *30* (6), 4717−4724.

(44) Chacón-Patiño, M. L.; Vesga-Martínez, S. J.; Blanco-Tirado, C.; Orrego-Ruiz, J. A.; Gómez-Escudero, A.; Combariza, M. Y. Exploring Occluded Compounds and Their Interactions with Asphaltene Networks Using High-Resolution Mass Spectrometry. *Energy Fuels* **2016**, *30* (6), 4550−4561.

(45) Rogel, E.; Ovalles, C.; Moir, M. Asphaltene Chemical Characterization as a Function of Solubility: Effects on Stability and Aggregation. *Energy Fuels* **2012**, *26* (5), 2655−2662.

(46) Chacón-Patiño, M. L.; Blanco-Tirado, C.; Orrego-Ruiz, J. A.; Gómez-Escudero, A.; Combariza, M. Y. High Resolution Mass Spectrometric View of Asphaltene−SiO2 Interactions. *Energy Fuels* **2015**, *29* (3), 1323−1331.

(47) Islam, A.; Cho, Y.; Yim, U. H.; Shim, W. J.; Kim, Y. H.; Kim, S. The comparison of naturally weathered oil and artificially photo-degraded oil at the molecular level by a combination of SARA fractionation and FT-ICR MS. *J. Hazard. Mater.* **2013**, *263* (2), 404−411.

(48) McKenna, A. M.; Nelson, R. K.; Reddy, C. M.; Savory, J. J.; Kaiser, N. K.; Fitzsimmons, J. E.; Marshall, A. G.; Rodgers, R. P. Expansion of the Analytical Window for Oil Spill Characterization by Ultrahigh Resolution Mass Spectrometry: Beyond Gas Chromatography. *Environ. Sci. Technol.* **2013**, *47* (13), 7530−7539.

(49) Altgelt, K. H.; Boduszynski, M. M. *Composition and Analysis of Heavy Petroleum Fractions*; Chemical Industries, 1994.

(50) Murray, J. A.; Sander, L. C.; Wise, S. A.; Reddy, C. M. *Gulf of Mexico Research Initiative 2014/2015 Hydrocarbon Intercalibration Experiment: Description and Results for SRM 2779 Gulf of Mexico Crude Oil and Candidate SRM 2777 Weathered Gulf of Mexico Crude Oil*; 2016.

(51) Krajewski, L. C.; Lobodin, V. V.; Robbins, W. K.; Jin, P.; Bota, G.; Marshall, A. G.; Rodgers, R. P. Method for Isolation and Detection of Ketones Formed from High-Temperature Naphthenic Acid Corrosion. *Energy Fuels* **2017**, *31* (10), 10674−10679.

(52) McLafferty, F. W. *Mass Spectrometry of Organic Ions*, 1st ed.; Academic Press, 1963.

(53) Smith, D. F.; Podgorski, D. C.; Rodgers, R. P.; Blakney, G. T.; Hendrickson, C. L. 21 T FT-ICR Mass Spectrometer for Ultrahigh-Resolution Analysis of Complex Organic Mixtures. *Anal. Chem.* **2018**, *90* (3), 2041−2047.

(54) Krajewski, L. C.; Rodgers, R. P.; Marshall, A. G. 126 264 Assigned Chemical Formulas from an Atmospheric Pressure Photoionization 9.4 T Fourier Transform Positive Ion Cyclotron Resonance Mass Spectrum. *Anal. Chem.* **2017**, *89* (21), 11318−11324.

(55) Stanford, L. A.; Rodgers, R. P.; Marshall, A. G.; Czarnecki, J.; Wu, X. A. Compositional Characterization of Bitumen/Water Emulsion Films by Negative- and Positive-Ion Electrospray Ionization and Field Desorption/Ionization Fourier Transform Ion Cyclotron Resonance Mass Spectrometry. **2007**, *21* (2), 963−972.

(56) Blakney, G. T.; Hendrickson, C. L.; Marshall, A. G. International Journal of Mass Spectrometry Predator data station: A fast data acquisition system for advanced FT-ICR MS experiments. *Int. J. Mass Spectrom.* **2011**, *306* (2−3), 246−252.

(57) Corilo, Y. E. *Omics LLC*: Tallahassee, FL, 2014.

(58) Ehrhardt, M. G.; Bícego, M. C.; Weber, R. R. Photo-oxidation of 1-methylnaphthalene dissolved in seawater and exposed to sunlight under quasi-environmental conditions. *J. Photochem. Photobiol., A* **1997**, *108*, 253−259.